Bimetallic Complexes from Amphoteric Group 13/15 Ligands: Syntheses and X-ray Crystal Structures

Florian Thomas,[a] Stephan Schulz,*[a] Martin Nieger,[a] and Kalle Nättinen[b]

Abstract: Bimetallic, pentel-bridged complexes of the type [(dmap)Me_2-M–E($SiMe_3$)$_2$–M′($CO)_n$] (M = Al, Ga; E = P, As, Sb; M′ = Cr, Fe, Ni; DMAP = 4-(dimethylamino)pyridine) are formed by reactions of DMAP-coordinated monomeric Group 13/15 compounds [(dmap)Me_2M–E($SiMe_3$)$_2$] with the transition metal complexes [(Me_3N)Cr($CO)_5$], [$Fe_3(CO)_{12}$], and [Ni($CO)_4$]. For the first time, this reaction offers a general pathway to compounds containing a Group 13 metal and a transition metal bridged by a pentel atom. Complexes prepared in this way were characterized by IR and multinuclear NMR spectroscopy and by single-crystal X-ray structure analysis. Their electronic and structural properties are discussed in detail. The Group 13/15 ligands are very weak π acceptors, which is likely to be due to the electropositive Group 13 metal, and the complexes feature comparatively long pentel–transition metal bonds. In addition, the synthesis and structural characterization of the parent DMAP-coordinated gallanes [(dmap)-Me_2Ga–E($SiMe_3$)$_2$] (E = P, As) are reported.

Keywords: bimetallic complexes · donor–acceptor systems · main group elements · transition metals

Introduction

In the last decade Group 13/15 compounds containing the higher homologues of Groups 13 (M = Al, Ga, In) and 15 (E = P, As, Sb, Bi) have been investigated in detail. The research interest was mainly focussed on heterocycles [R_2M–ER'_2]$_x$ (R, R′ = organic ligands, x = 2, 3) or Lewis acid/base adducts [R_3M ← ER'_3] due to their potential to serve as single-source precursors for the preparation of III/V semiconductor layers by MOCVD processes (*metal organic chemical vapor deposition*).[1] In addition, monomeric Group 13/15 compounds R_2M–ER'_2 and RM–ER′ (R, R′ = bulky ligands) have been investigated in detail in order to estimate the amount of π bonding between the adjacent donor and acceptor centers.[2]

However, the chemical reactivity of Group 13/15 compounds has been studied to a far lesser extent. Considering the lability of the dative M ← E bond in Lewis acid/base adducts [R_3M ← ER'_3] and the small number of heterocycles or -cubanes [RM–ER′]$_x$ (x = 2–4) containing the heavier elements of Group 15, compounds of the general formula [R_2M–ER'_2]$_x$ (x = 1–3) seem to be the most suitable starting materials for further reactivity studies. The central R_2M–ER'_2 fragment possesses an "amphoteric character", since it can act simultaneously as Lewis acid and Lewis base (Scheme 1).[3] This feature allows two basic reactions in coordination chemistry: the coordination of Group 13 compounds to Lewis bases and the reaction of Group 15 compounds as ligands in transition metal complexes.

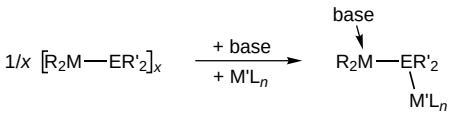

Scheme 1. Amphoteric character of the Group 13/15 fragment R_2M–ER'_2.

The bimetallic complex [Me_3N(Me_3SiCH_2)$_2$Al–P(Ph_2)–Cr($CO)_5$], synthesized by Beachley et al. by a particular ring cleavage reaction of the heterocycle [(Me_3SiCH_2)$_2$AlPPh_2]$_2$ and [(Me_3N)Cr($CO)_5$], was the first example of such a compound, in which both coordination modes are present.[3] Unfortunately, this type of reaction succeeded only in very few cases, and no other compound could be characterized by X-ray structure analysis.[4] The authors suggested that the reactivity of Group 13/15 heterocycles towards ring cleavage reactions depends on both the degree of association of the heterocycle in solution and the Lewis acidity of the triel atom.

[a] Priv.-Doz. Dr. S. Schulz, Dipl.-Chem. F. Thomas, Dr. M. Nieger
Institut für Anorganische Chemie der Universität Bonn
Gerhard-Domagk-Strasse 1, 53121 Bonn (Germany)
Fax: (+49) 228-73-5927
E-mail: sschulz@uni-bonn.de

[b] K Nättinen
Department of Organic Chemistry
University of Jyväskylä, PO Box 35
40101 Jyväskylä (Finland)

  0947-6539/02/0808-1915 $ 20.00+.50/0

However, no straight relationship could be proved in further studies.[4] In addition, only reactions with $[(Me_3N)Cr(CO)_5]$ were successful, whereas other transition metal complexes such as $[Cr(CO)_6]$ or $[(thf)Cr(CO)_5]$ failed to give the desired bimetallic complexes. We thus were interested in the development of a more general approach to this particular class of compounds. Our intention was to elude the necessity to employ reagents containing both the Lewis base and the transition metal fragment in one molecule by splitting up the synthesis in a two-step reaction. For this purpose we developed a general synthetic pathway to Lewis base stabilized, monomeric Group 13/15 compounds.[5] Heterocycles $[R_2M{-}E(SiMe_3)_2]_x$ are cleaved by the strong Lewis base 4-(dimethylamino)pyridine (DMAP) to yield monomers of the type $[(dmap)R_2M{-}E(SiMe_3)_2]$ (M = Al, Ga; E = P, As, Sb, Bi; R = Me, Et) containing a pentel center with the coordination number 3. Consequent reactions of monomeric Group 15 alanes $[(dmap)Me_2Al{-}E(SiMe_3)_2]$ (E = P, As, Sb) prepared in this way with nickel tetracarbonyl led to pentel-bridged bimetallic complexes $[(dmap)Me_2Al{-}E(SiMe_3)_2{-}Ni(CO)_3]$, clearly demonstrating the availability of the *lone pair* for further complexation reactions.[6] In order to verify the generality of our approach to form also complexes with other transition metals and to investigate the influence of the Group 13 metal on the structure of such complexes, we conducted reactions of different monomers (with M = Al, Ga; E = P, As, Sb) with several transition metal carbonyls (M′ = Cr, Fe, Ni), which are presented herein. For this purpose, we synthesized two new Ga-containing DMAP-coordinated monomers $[(dmap)Me_2Ga{-}E(SiMe_3)_2]$ (E = P, As), the syntheses and structural characterizations of which are also reported.

Results and Discussion

Reactions of 4-(dimethylamino)pyridine (DMAP) with gallium-Group 15 heterocycles $[Me_2GaE(SiMe_3)_2]_2$ in a 2:1 molar ratio lead to the formation of the corresponding Lewis base stabilized monomers $[(dmap)Me_2Ga{-}E(SiMe_3)_2]$ (E = P **1**, As **2**, Scheme 2).

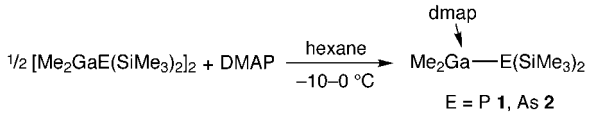

Scheme 2. Synthesis of the DMAP-coordinated monomers **1** and **2**.

Compounds **1** and **2** are isolated in good yields as colorless to light yellow crystals from solutions in hexane at −30 °C. The compounds are very sensitive towards oxygen and moisture both in solution and in the solid state. Unlike the corresponding aluminum compounds $[(dmap)Me_2Al{-}E(SiMe_3)_2]$,[5] **1** and **2** can be kept at room temperature only for short periods of time and form insoluble decomposition products within an hour. Initial studies indicate the corresponding In compounds to be even more temperature labile.[7] NMR spectra of **1** and **2** show the expected resonances due to the organic ligands. As was found for the corresponding alanes, the ligands bound to the triel and pentel atom experience a downfield shift compared with the corresponding heterocycles, and the protons of the coordinated DMAP molecule an upfield shift compared with free DMAP.[5] Single crystals of **1** and **2** suitable for X-ray structure analysis were obtained at −30 °C from solutions in hexane; Figures 1 and 2 show their molecular structures. Selected bond lengths and angles are summarized in Table 1.

Table 1. Selected bond lengths [pm] and angles [°] of the DMAP-coordinated monomers **1** and **2**.

	1	**2**
M–E	237.2(1)	245.5(1)
M–N	208.0(2)	208.2(2)
∅ M–C	198.5	198.2
∅ E–Si	224.4	234.3
C–M–C	118.9(2)	119.7(2)
N–M–E	104.7(1)	104.3(1)
Si–E–Si	103.9(1)	101.8(1)

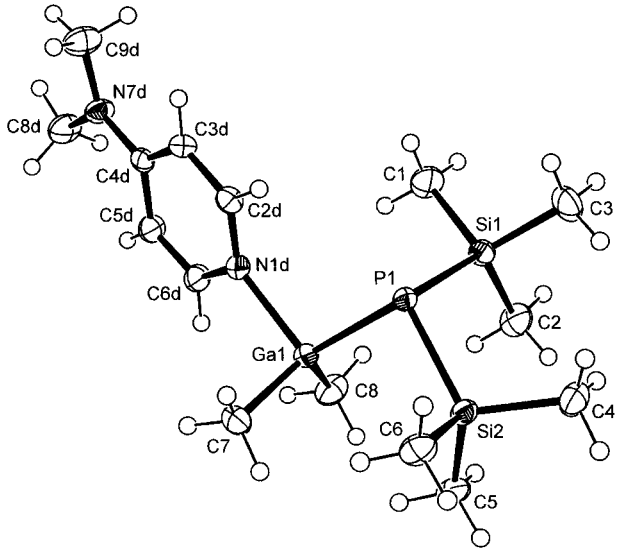

Figure 1. ORTEP diagram (50% probability ellipsoids) showing the solid-state structure and atom-numbering scheme of **1**.

Compounds **1** and **2** crystallize in the monoclinic space groups $P2_1/n$ and $P2_1/c$ (no. 14), respectively. They are not isostructural to the analogous aluminum derivatives, which crystallize with two independent molecules in the asymmetric unit,[5c] but to the aluminum stibide and bismuthide $[(dmap)Me_2Al{-}E(SiMe_3)_2]$ (E = Sb, Bi).[5a, b] The average Ga–C (**1**: 198.4 pm; **2**: 198.2 pm) and E–Si bond lengths (**1**: 224.4 pm; **2**: 234.3 pm) are within the expected range and remain nearly unchanged compared with the starting heterocycles.[8] The slight shortening of the E–Si bond lengths is accompanied with a decrease of the Si–E–Si bond angle and is a result of the reduced coordination number of the pentel center (c.n. 4 → 3). As was observed for the aluminum derivatives $[(dmap)Me_2Al{-}E(SiMe_3)_2]$ (E = P, As),[5c] the central Ga–E bonds (**1**: 237.2(1) pm; **2**: 245.5(1) pm) are

  0947-6539/02/0808-1916 $ 20.00+.50/0 *Chem. Eur. J.* **2002**, *8*, No. 8

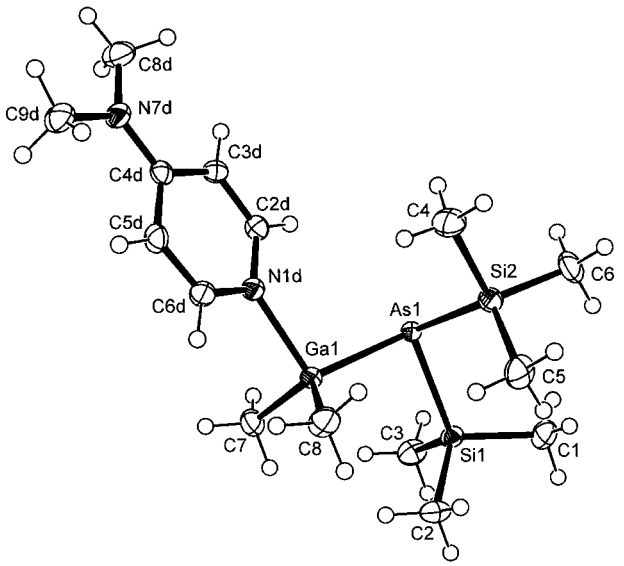

Figure 2. ORTEP diagram (50% probability ellipsoids) showing the solid-state structure and atom-numbering scheme of **2**.

relatively short (typical range 230–255 pm for Ga–P; 240–260 pm for Ga–As)[9] and noticeably shortened by about 7 pm compared with the corresponding heterocycles. This observation reflects the minor steric strain of the Lewis base coordinated monomers. The Ga–E bond lengths are somewhat shorter (0.5–1.5 pm) than those for the corresponding Al–E bonds, and this is frequently observed for Group 13/15 heterocycles despite the nearly identical covalent radii of both elements (Al: 125 pm; Ga: 126 pm).[10] The most striking difference between the Ga and the Al derivatives is the length of the dative M ← N bond. The Ga–N bonds (**1**: 208.0(2) pm; **2**: 208.2(2) pm) are elongated by about 10 pm, reflecting the decreased Lewis acidity. This is in accordance with experimental findings for compounds containing dative Al ← N and Ga ← N bonds, generally showing differences of 7–10 pm (e.g. [$H_3M \leftarrow$ quinuclidine]: M = Al 199.1 pm, M = Ga 206.3 pm;[11] [tmeda · $2MMe_3$]: M = Al 207.5 pm, M = Ga 217.4 pm,[12] tmeda = tetramethylethylenediamine). Comparable Ga–N bond lengths were reported for gallane/pyridine adducts such as [$Me_2Ga(Cl) \leftarrow$ 2-(methylamino)pyridine] (206.6(3) pm).[13] In agreement with the concept proposed by Haaland, the weakness of the dative Ga ← N bond leads to a more planar geometry around the triel atom.[14] The sum of the bond angles around M (C–M–C and C–M–E) are 347.4° (**1**) and 347.2° (**2**), respectively, whereas for the corresponding alanes values between 340–343° were found.[5]

The DMAP-coordinated monomers [(dmap)Me_2M–$E(SiMe_3)_2$] (M = Al, E = P, As; M = Ga, E = P **1**, As **2**, Sb) were used as starting compounds for reactions with different transition metal complexes. We performed reactions of the Al-containing monomers with [$(Me_3N)Cr(CO)_5$], [$Fe_3(CO)_{12}$], and [$Ni(CO)_4$] in order to study the influence of the specific transition metal. The Ga-containing monomers were treated with [$Ni(CO)_4$] to allow comparisons with previously published aluminum-containing complexes [(dmap)Me_2Al–$E(SiMe_3)_2$–$Ni(CO)_3$] (E = P, As, Sb).[6] Scheme 3 summarizes the experiments. All compounds were characterized by IR and multinuclear NMR spectroscopy and, except for **7**, by single-crystal X-ray structure analysis. Even if the gallium–pentel–transition metal complexes **7**–**9** seem to be more temperature stable compared with the corresponding Ga–pentel monomers **1** and **2**, they should be stored at −30 °C under an inert gas atmosphere. At ambient temperature, decomposition occurs within several days, evidently due to the loss of the transition metal fragment. These findings, which were also observed for the alane–pentel–transition metal complexes **3**–**6**, agree with the results obtained from mass spectroscopy studies. We were not able to detect the molecular ion peak for any of the transition metal complexes **3**–**9**. The signals with the highest mass observed correspond to the transition metal fragment and the main group ligand fragment, respectively. Therefore, no high-resolution mass spectra of **3**–**9** can be presented.

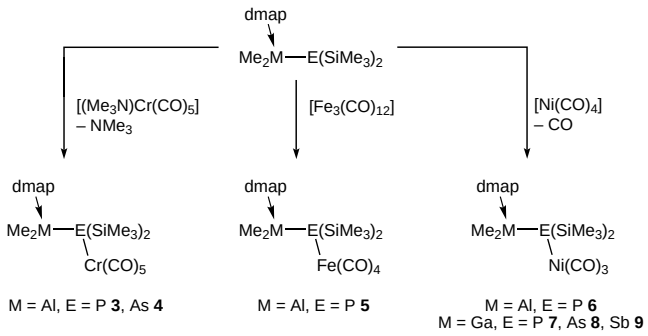

Scheme 3. Reactions of DMAP-coordinated monomers with different transition metal complexes.

Chromium complexes: Reactions of [(dmap)Me_2Al–$E(SiMe_3)_2$] with [$(Me_3N)Cr(CO)_5$] in refluxing hexane lead to the formation of the bimetallic chromium complexes [(dmap)Me_2Al–$E(SiMe_3)_2$–$Cr(CO)_5$] (E = P **3**, As **4**) under elimination of NMe_3. The products precipitate from solutions in hexane as yellow to reddish powders which can be recrystallized from CH_2Cl_2 yielding yellow crystals of X-ray quality. IR and ^{13}C NMR spectra confirm the presence of the chromium pentacarbonyl fragment. As was expected from previous studies, the CO vibrational bands in the arsenic-bridged complex **4** are shifted to lower wavenumbers (**3**: 1929, 2027, 2056 cm^{-1}; **4**: 1921, 2025, 2044 cm^{-1}), and the ^{13}C NMR resonances shifted to lower field (**3**: δ = 217.8, 223.7; **4**: δ = 219.7, 225.1) compared with the phosphorus-bridged complex **3**, indicating an increased σ-donor/π-acceptor ratio with increased atomic number of the pentel center.[6,15] Figures 3 and 4 show the molecular structures of **3** and **4** as obtained from single-crystal X-ray structure analysis (see Table 2 for selected bond lengths and angles). The compounds are isomorphous and crystallize in the triclinic space group $P\bar{1}$ (no. 2).

Compounds **3** and **4** adopt a distorted staggered conformation along the Al–E bond with N–Al–E–Cr torsion angles of 36.9(1)° (**3**) and 37.6(1)° (**4**), respectively. The conformation is dominated by steric interactions between the DMAP pyridine ring and the bulky $Cr(CO)_5$ fragment, leading to a severe

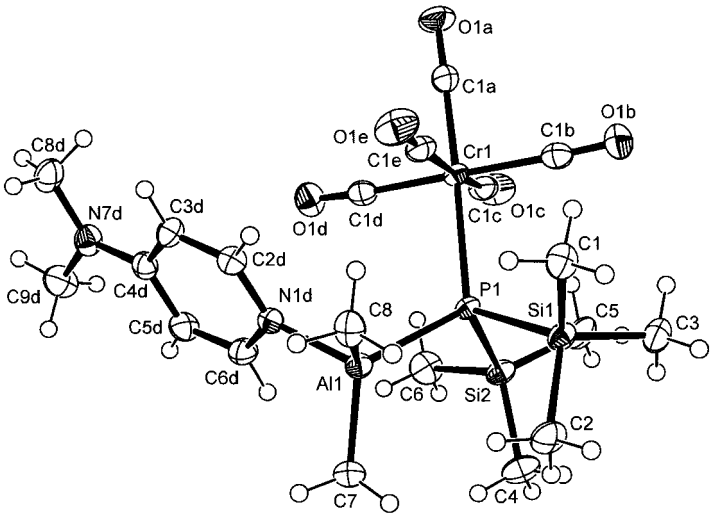

Figure 3. ORTEP diagram (50% probability ellipsoids) showing the solid-state structure and atom-numbering scheme of **3**.

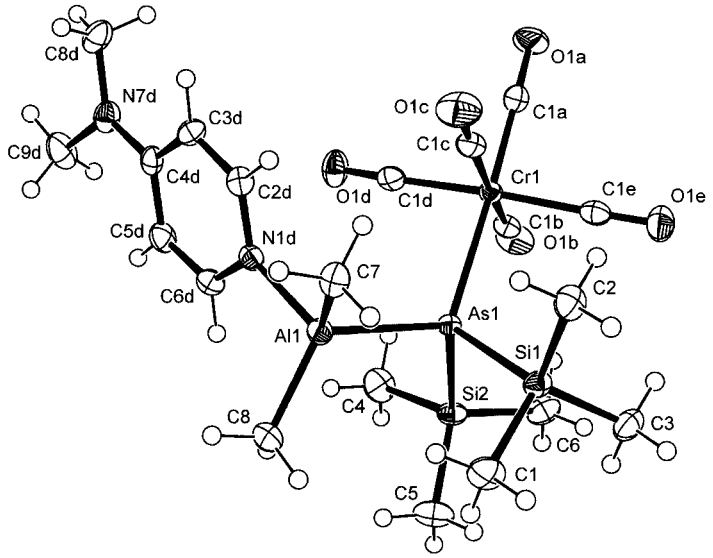

Figure 4. ORTEP diagram (50% probability ellipsoids) showing the solid-state structure and atom-numbering scheme of **4**.

deformation of the $[(L)Cr(CO)_5]$ octahedron. In both cases the Cr–E bonds (**3**: 252.8(1) pm; **4**: 260.0(1) pm) belong to the longest bonds found for $E–Cr(CO)_5$ fragments so far (typical range for E = P: 224–258 pm; E = As: 237–263 pm;[9] cp. 242.2 pm for $[(Ph_3P)Cr(CO)_5]$ and 249.7 pm for $[(Ph_3As)Cr(CO)_5)]$.[16] To the best of our knowledge only the metalloarsaalkene $[(Me_2N)_2C{=}As\{Fe(CO)_2Cp\}\{Cr(CO)_5\}]$ features a longer $As–Cr(CO)_5$ bond (262.8(1) pm).[17] In combination with the rather short Cr–CO(*trans*) bond lengths (**3**: 184.4(2) pm; **4**: 183.7(2) pm, the typical range for $[(R_3E)Cr(CO)_5]$: 180–192 pm),[9] these results indicate a comparatively weak $Cr \rightarrow E$ π back bonding.[18] Both the Al–E (**3**: 242.8(1) pm; **4**: 251.2(1) pm) and the E–Si bonds (**3**: 226.7 pm; **4**: 235.9 pm; averages) are elongated compared with the uncomplexed monomers, and this is caused by the increase in coordination number from 3 to 4 and the steric interactions with the bulky $Cr(CO)_5$ fragment. As expected the effect is more distinct on the somewhat smaller phosphorus atom (covalent radii 110 pm vs. 121 pm for arsenic).[10] The considerable elongation of the Al–E bonds by 5.1 pm (**3**) and 4.1 pm (**4**), respectively, is accompanied by a shortening of the Al–N bonds, whereas the Al–C bond lengths remain nearly unchanged. The similar complex $[Me_3N(Me_3SiCH_2)_2Al–P(Ph_2)–Cr(CO)_5]$[3] shows some characteristic differences when compared with **3**. The Al–P (248.5(1) pm) and Al–N bond lengths (204.9(3) pm) are rather long, while the P–Cr bond length (248.2(1) pm) is significantly shorter. These structural differences reflect the contrary environments around the central atoms M and E in the two complexes, that is, the sterically more demanding substituents are located on the triel center (Beachley: NMe_3, CH_2SiMe_3) and on the pentel center (**3**: $SiMe_3$), respectively.

Iron complex: The reaction of $[(dmap)Me_2Al–P(SiMe_3)_2]$ with $[Fe_3(CO)_{12}]$ in hexane leads to the formation of $[(dmap)Me_2Al–P(SiMe_3)_2–Fe(CO)_4]$ (**5**). A considerable amount of a dark red by-product subsides from the solution, which could not be characterized so far. IR and ^{13}C NMR spectra confirm the presence of the iron tetracarbonyl fragment in the product. The presence of three IR bands in the carbonyl region (1911, 1956, 2008 cm^{-1}) points to a local C_{3v} symmetry of the complex, which requires an axial position of the Group 13/15 ligand.

Single crystals of X-ray quality were obtained from solutions in hexane at −60 °C. Figure 5 shows the molecular structure of **5** obtained by X-ray structure analysis (see Table 2 for selected bond lengths and angles). Compound **5** crystallizes in the triclinic space group $P\bar{1}$ (no. 2). The molecule adopts a distorted staggered conformation along the Al–P bond very similar to that for **3** with an N–Al–P–Fe torsion angle of 34.1(1)°. Again, steric interactions be-

Table 2. Selected bond lengths [pm] and angles [°] of the bimetallic complexes **3**, **4**, **5**, **6** (averages), **8**, and **9**.

	3	**4**	**5**	**6**	**8**	**9**
E–M′	252.8(1)	260.0(1)	237.7(1)	231.5	241.9(1)	255.4(1)
M′–CO[a]	184.4(3)	183.7(2)	177.0(2)	177.6	179.0	178.2
C–O[b]	115.6(3)	115.5(2)	114.7(2)	113.9	113.8	114.7
M–E	242.8(1)	251.2(1)	243.2(1)	240.0	246.4(1)	264.7(1)
M–N	196.3(2)	195.5(2)	196.1(1)	196.0	204.5(2)	204.6(2)
∅ M–C	197.0	197.0	196.9	197.2	197.9	197.8
∅ E–Si	226.7	235.9	227.3	224.3	234.9	254.9
C–M–C	118.9(2)	120.1(1)	116.5(1)	118.0	119.6(1)	120.3(1)
N–M–E	107.1(1)	106.0(1)	102.8(1)	104.5	101.0(1)	100.0(1)
Si–E–Si	102.9(1)	102.31(1)	105.9(1)	107.0	105.9(1)	104.2(1)
M–E–M′	116.9(1)	117.2(1)	114.4(1)	116.7	120.2(1)	123.2(1)
∅ E–M′–CO (*cis*)	92.0	91.1	89.6	106.2	104.9	103.2

[a] M′–CO(*trans*) for **3**, **4**, and **5**, average M′–CO for **6**, **8**, and **9**. [b] C–O(*trans*) for **3**, **4**, and **5**, average C–O for **6**, **8**, and **9**.

0947-6539/02/0808-1918 $ 20.00+.50/0 *Chem. Eur. J.* **2002**, *8*, No. 8

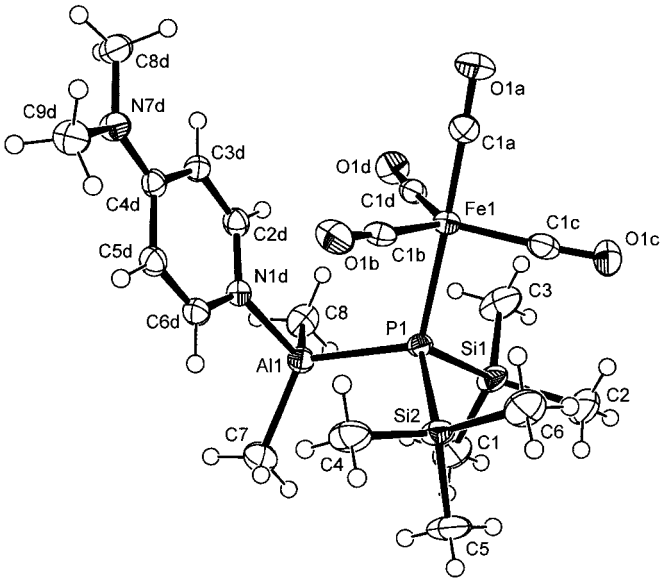

Figure 5. ORTEP diagram (50% probability ellipsoids) showing the solid-state structure and atom-numbering scheme of **5**.

tween the DMAP pyridine ring and the $Fe(CO)_4$ group are decisive factors. The four CO ligands and the Group 13/15 ligands form a moderately distorted trigonal bipyramid around the iron center. In agreement with the observations in solution, the phosphorus atom occupies an axial position, which is preferred by ligands with strong σ-donor and weak π-acceptor abilities.[19] As was found for the chromium complex **3** the P–M′ interaction (M′ = transition metal) in **5** seems rather weak, and this leads to the longest P–$Fe(CO)_4$ bond (237.7(1) pm) reported so far (observed range for pentacoordinated iron: 216–237 pm).[9] For the related complex [{$(Me_3Si)_3$P}$Fe(CO)_4$] a P–Fe bond length of 233.8(4) pm was found. A CSD database search confirmed only one compound containing a phosphorus atom bound to a terminal iron complex that featured a longer P–Fe bond.[20] The other central structural parameters of **5** are very similar to those of the chromium complex **3**, the Al–P (243.2(1) pm) and P–Si bonds (av. 227.3 pm) being slightly longer and the Al–N bond (196.1(1) pm) slightly shorter.

Nickel complexes: The synthesis of [(dmap)Me_2Al–P$(SiMe_3)_2$–Ni$(CO)_3$] (**6**) has already been published, but its molecular structure was not determined due to disorder problems.[6] We now obtained single crystals of X-ray quality from solutions in cyclohexane. Compound **6** crystallizes in the triclinic space group $P\bar{1}$ with six independent molecules in the asymmetric unit. For clarity, Figure 6 displays the molecular structure of only one independent molecule (see Table 2 for averages of selected bond lengths and angles).

The six independent molecules cover a wide range of conformations with N–Al–P–Ni torsion angles between 22 and 88°. This is in sharp contrast to the nearly accurate staggered conformation found in the homologous arsane and stibane complexes.[6] The four ligands around the nickel center form a distorted tetrahedron with the three CO ligands bent towards the phosphorus atom (av. P–Ni–C angle: 106.2°). Again the P-transition metal bond is very long. The average P–Ni bond length of 231.5 pm is about 2 pm longer than in [(tBu$_3$P)Ni$(CO)_3$], which already contains a sterically hindered and weak π-accepting phosphane ligand.[21] This compound forms the reference for the electronic Tolman parameter χ for a given ligand L, defined as the difference of the wavenumbers of the A_1 vibrations for a nickel carbonyl complex [(L)Ni$(CO)_3$] compared with [(tBu$_3$P)Ni$(CO)_3$].[22] Examples of χ values are 13.25 for PPh_3 and 0.8 for the weak π-acceptor P$(SiMe_3)_3$.[23] According to this concept, a negative value of $\chi = -8$ is to be assigned to the ligand [(dmap)Me_2Al–P$(SiMe_3)_2$] since its Ni$(CO)_3$ complex exhibits an A_1 vibration ($\nu = 2048$ cm^{-1}) shifted to a wavenumber below 2056.1 cm^{-1}. Thus the π-acceptor ability of this particular ligand should be extremely weak, which agrees with the aforementioned observations made for the chromium and iron complexes. The phosphorus/transition metal interaction has almost exclusively P → M′ σ-dative character. Evidently the highly electropositive Group 13 metal (electronegativity of Al: 1.47)[24] in combination with the two $SiMe_3$ groups strongly increases the electron density on the pentel center, and this renders additional π back donation from the transition metal improbable. Similarly to the phosphorus complexes **3** and **5**, but in contrast to the homologous complexes [(dmap)Me_2Al–E$(SiMe_3)_2$–Ni$(CO)_3$] (E = As, Sb)[6] the Al–P bonds are slightly elongated upon coordination to the transition metal fragments by about 2 pm (av. 240.0 pm), accompanied by a shortening of the Al–N bonds (av. 196 pm). Evidently due to the smaller phosphorus atom, steric interactions between the substituents and the transition metal fragment are more

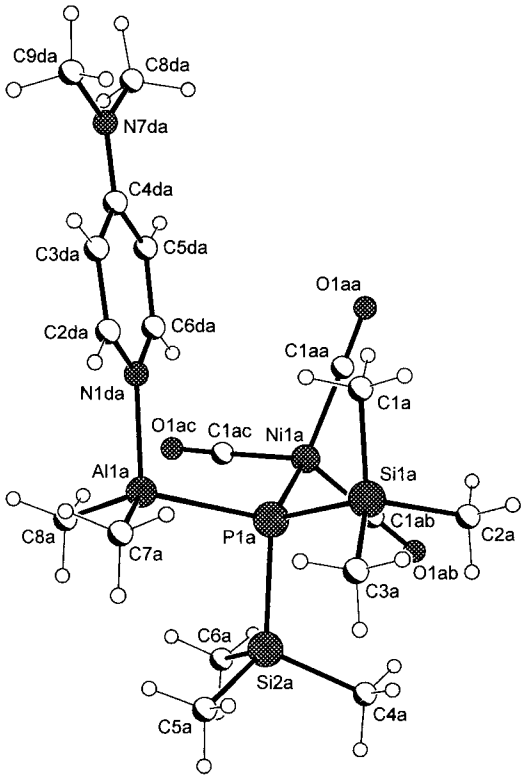

Figure 6. Ball-and-stick diagram showing the solid-state structure and atom-numbering scheme of **6**; for clarity, only one independent molecule of the asymmetric unit is presented.

interfering than those for the larger homologues of Group 15. The bond lengths to the remaining ligands bound to the triel and pentel centers (Al–C 197.2 pm, P–Si 224.3 pm, averages) do not show significant changes compared with those for the uncomplexed monomer. In contrast, the bond angles around the pentel center undergo significant change, especially when compared with **3** and **5**. The sum of the bond angles around the phosphorus center (Si–P–Si and Al–P–Si) of the ligand increases from 309.8° in the uncomplexed monomer (pyramidal phosphorus)[5c] to 321.1° (average) in **6** (tetrahedral environment). In the complexes **3** ($\Sigma = 313.4°$) and **5** ($\Sigma = 318.9°$), the increase of the bond angles is much smaller and reflects the different steric demand of the transition metal fragments $Cr(CO)_5 > Fe(CO)_4 > Ni(CO)_3$. The sterically crowded compound **3** shows nearly the same pyramidalization as the free ligand.

In an extensive ^{13}C NMR study on more than 100 transition metal complexes $[(R_3E)M'(CO)_n]$ (E = Group 15 element), Bodner et al. observed that the variation of the organic ligands on the pentel center usually had a larger effect on the carbonyl resonances than variation of the pentel center itself.[15] We therefore studied the reactions of the monomeric Group 15 gallanes $[(dmap)Me_2Ga–E(SiMe_3)_2]$ (E = P **1**, As **2**, Sb) with nickel tetracarbonyl to determine the influence of the Group 13 metal by comparison with the analogous aluminum compounds. Due to the temperature sensitivity of the gallane monomers, $[Ni(CO)_4]$ was added at 0 °C, and the reaction mixture slowly warmed to ambient temperature. Under elimination of carbon monoxide, the tricarbonyl nickel complexes $[(dmap)Me_2Ga–E(SiMe_3)_2–Ni(CO)_3]$ (E = P **7**, As **8**, Sb **9**) were obtained in good yields. IR and ^{13}C NMR spectra confirm the presence of the $Ni(CO)_3$ fragment in the products.[25] The differences between the individual A_1 IR stretching frequencies and ^{13}C chemical shifts (see Table 3) as well as the differences between the respective aluminum compounds are very small, but a general tendency is evident. All compounds show very low wavenumbers of the A_1 vibration leading to negative electronic Tolman parameters χ between −6 and −14. The σ-donor/π-acceptor ratio increases with the pentel center E in the order P < As < Sb and, as was expected due to the different electronegativities of the triel (Al: 1.47, Ga: 1.82),[24] is larger for Al than for Ga.

Single crystals of **7**–**9** were obtained from solutions in pentane at −30 °C. Compounds **8** and **9** crystallize in the triclinic space group $P\bar{1}$ and are isostructural to the analogous aluminum compounds $[(dmap)Me_2Al–E(SiMe_3)_2–Ni(CO)_3]$ (E = As, Sb).[6] Figures 7 and 8 show the molecular structures of the compounds (see Table 2 for selected bond lengths and angles). They represent the first structurally characterized examples of bimetallic complexes with a pentel center bridging a transition metal and gallium.[4] The structure of **7** could not be determined due to disorder problems.

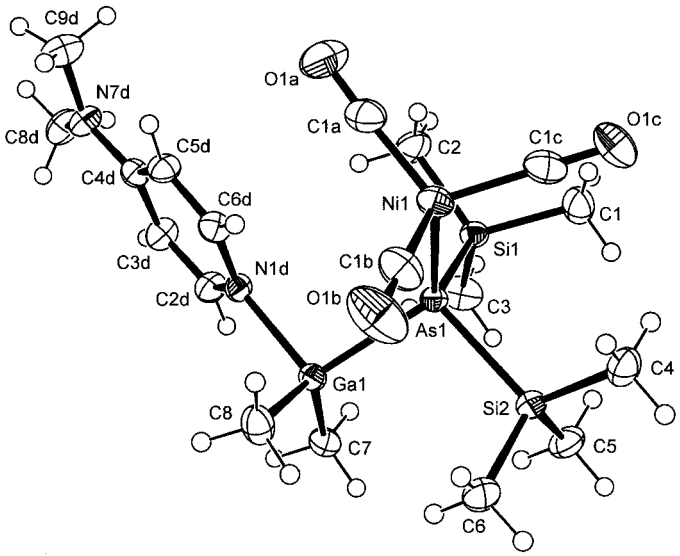

Figure 7. ORTEP diagram (50% probability ellipsoids) showing the solid-state structure and atom-numbering scheme of **8**.

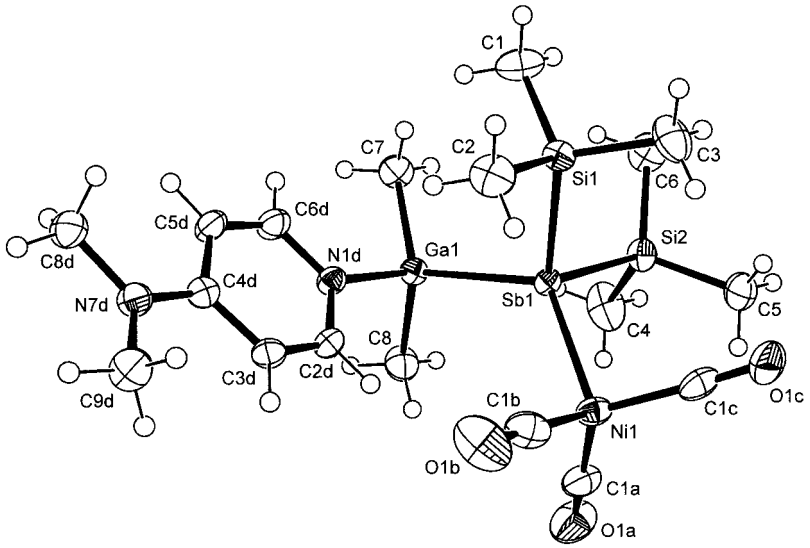

Figure 8. ORTEP diagram (50% probability ellipsoids) showing the solid-state structure and atom-numbering scheme of **9**.

Table 3. CO stretching vibrations [A_1 band, cm^{-1}], ^{13}C chemical shifts [δ], and electronic Tolman parameters[22] of complexes $[(dmap)Me_2M–E(SiMe_3)_2–Ni(CO)_3]$.

M/E	Al/P	Al/As	Al/Sb	Ga/P **7**	Ga/As **8**	Ga/Sb **9**
ν(CO)	2048	2046	2042	2050	2048	2044
δ(CO)	199.5	199.8	200.9	199.5	199.6	200.7
χ	−8	−10	−14	−6	−8	−12

0947-6539/02/0808-1920 $ 20.00+.50/0 *Chem. Eur. J.* **2002**, *8*, No. 8

The molecules adopt *gauche* conformations along the Ga–E bond with N–Ga–E–Ni torsion angles near 60° (**8**: 66.2(1)°; **9**: 64.3(1)°). The ligands around the nickel center form a tetrahedron that is increasingly distorted with increasing atomic number of the pentel center (average E–Ni–C angle **8**: 104.9°; **9**: 103.2°; cp. **6** (E = P): 106.2°). The bond lengths around the nickel center are hardly influenced by the exchange of the triel atom. The E–Ni (E = As **8**: 241.9(1) pm; E = Sb **9**: 255.4(1) pm), Ni–C (**8**: 170.9 pm; **9**: 113.8 pm), and C–O bond lengths (**8**: 113.8 pm; **9**: 114.7 pm) are virtually unchanged compared with those for the respective aluminum compounds. In contrast to all above-mentioned complexes, the Ga–E bonds of **8** (246.4(1) pm) and **9** (264.7(1) pm) as well as the E–Si bonds (**8**: 234.9 pm; **9**: 254.9 pm) are not elongated upon complexation.[26] This leads to the conclusion that steric interactions are negligible when the transition metal fragment is relatively small and the pentel centers possess sufficiently large atomic radii. Another interesting feature is the shortening of the Ga–N bonds by 3.7 pm (**8**: 204.5(2) pm) and 2 pm (**9**: 204.6(2) pm), respectively, even if the Ga–E bonds remain almost unchanged. The reason behind this effect is still unclear.

Conclusion

The two-step synthesis consisting of a ring cleavage reaction of Group 13/15 heterocycles with the Lewis base DMAP followed by complexation of the resulting DMAP-coordinated monomers with transition metal complexes offers a general pathway to pentel-bridged bimetallic complexes of the type [(base)R_2M–E(R'_2)–M′$(CO)_n$] (M = Group 13 metal, E = pentel, M′ = transition metal). Complexes with different Group 13 metals (Al, Ga), pentels (P, As, Sb), and transition metals (Cr, Fe, Ni) were obtained in this way. A closer investigation of the structural and electronic properties of the Group 13/15 ligands by X-ray structure analysis and IR spectroscopy indicates that steric interactions are especially important in the phosphorus complexes with the bulkier $Fe(CO)_4$ and $Cr(CO)_5$ fragments, whereas they are less important for the higher pentels As and Sb. The π-acceptor abilities of the ligands generally seem to be very weak, and the σ-donor/π-acceptor ratio increases in the series P < As < Sb. The exchange of the Group 13 metal from Al to Ga induces only small changes in structural and electronic parameters. The Ga–E bonds are slightly shorter than the corresponding Al–E bonds, whereas the Ga–N bonds are significantly longer than the Al–N bonds. The gallane monomers are comparable weak π acceptors, and the σ-donor/π-acceptor ratio just slightly decreases from Al to Ga.

Experimental Section

General: All manipulations were performed in a glove box under an Ar atmosphere or by standard Schlenk techniques. Solvents were distilled from sodium benzophenone ketyl or Na/K alloy prior to use. [Me_2Ga-P($SiMe_3$)$_2$]$_2$,[8a, b] [Me_2GaAs($SiMe_3$)$_2$]$_2$,[8c] [(dmap)Me_2Al–P($SiMe_3$)$_2$], [(dmap)Me_2Al–As($SiMe_3$)$_2$], [(dmap)Me_2Ga–Sb($SiMe_3$)$_2$],[5c] and [(Me_3N)Cr$(CO)_5$][27] were prepared by literature methods. Compounds 4-(dimethylamino)pyridine (Merck) and $[Ni(CO)_4]$ (Strem Chemicals) were commercially available and used as received. $[Fe_3(CO)_{12}]$ (Aldrich) was dried in vacuum to remove protecting methanol before use. NMR spectra were recorded using a Bruker DPX300 spectrometer. ^{1}H and ^{13}C{^{1}H} spectra were referenced to the resonances of the solvents C_6D_6 (^{1}H $\delta = 7.15$; ^{13}C $\delta = 128.0$), [D_8]toluene (^{1}H $\delta = 7.09$; ^{13}C $\delta = 137.5$), and CD_2Cl_2 (^{1}H $\delta = 5.32$; ^{13}C $\delta = 53.8$). ^{31}P{^{1}H} spectra were referenced to external H_3PO_4 (^{31}P $\delta = 0$). Infrared spectra were recorded from solutions in pentane or CH_2Cl_2 between KBr plates by using a Nicolet Magna 550 FT-IR spectrometer. Melting points were measured in wax-sealed capillaries and were not corrected. Several attempts to obtain reliable elemental analyses failed. Both the Ga monomers **1** and **2** and the transition metal complexes **3**–**9** are very sensitive toward air and moisture, and this prevented them from being transferred without any decomposition into the analyzer. Therefore, several analyses (between three and four for each compound) showed significant variations with respect to their C and H contents.

General preparation of [(dmap)Me_2Ga–E($SiMe_3$)$_2$]: At −10 °C, 4-(dimethylamino)pyridine (2.0 mmol, 0.24 g) was added to a solution of the corresponding heterocycle (1.0 mmol, [Me_2GaP($SiMe_3$)$_2$]$_2$: 0.55 g; [Me_2GaAs($SiMe_3$)$_2$]$_2$: 0.64 g) in hexane (30 mL). The resulting suspension was slowly warmed to 0 °C over 2–3 h. After filtration, the resulting clear solution was concentrated to 15 mL and stored at −30 °C for 24 h. The compounds were obtained as colorless to light yellow crystals, which slowly decomposed at room temperature.

[(dmap)Me_2Ga–P($SiMe_3$)$_2$] (1): Colorless crystals, yield: 0.72 g (1.6 mmol, 81 %); m.p. 50–52 °C; ^{1}H NMR (300 MHz, C_6D_6, 30 °C): $\delta = 0.33$ (d, $^3J_{PH} = 1.9$ Hz, 6H; $GaMe_2$), 0.54 (d, $^3J_{PH} = 4.0$ Hz, 18H; $SiMe_3$), 1.96 (s, 6H; NMe_2), 5.66 (d, $^3J_{HH} = 6.8$ Hz, 2H; C(3d)–H), 8.24 (dd, $^3J_{HH} = 5.6$ Hz, $^4J_{HH} = 1.5$ Hz, 2H; C(2d)–H); ^{13}C{^{1}H} NMR (75.5 MHz, [D_8]toluene, −10 °C): $\delta = -1.1$ (d, $^2J_{PC} = 10.7$ Hz; $GaMe_2$), 5.8 (d, $^2J_{PC} = 10.3$ Hz; $SiMe_3$), 38.5 (NMe_2), 106.8 (C(3d)–H), 147.3 (C(2d)–H), 155.0 (C(4d)); ^{31}P NMR (121.5 MHz, C_6D_6, 30 °C): $\delta = -273.8$.

[(dmap)Me_2Ga–As($SiMe_3$)$_2$] (2): Light yellow crystals, yield: 0.68 g (1.7 mmol, 85 %); m.p. 58–61 °C; ^{1}H NMR (300 MHz, [D_8]toluene, −10 °C): $\delta = 0.38$ (s, 6H; $GaMe_2$), 0.63 (s, 18H; $SiMe_3$), 1.99 (s, 6H; NMe_2), 5.58 (d, $^3J_{HH} = 5.8$ Hz, 2H; C(3d)–H), 8.15 (d, $^3J_{HH} = 5.7$ Hz, 2H; C(2d)–H); ^{13}C{^{1}H} NMR (75.5 MHz, [D_8]toluene, −10 °C): $\delta = 4.6$ ($GaMe_2$), 6.1 ($SiMe_3$), 38.5 (NMe_2), 106.9 (C(3d)–H), 147.2 (C(2d)–H), 155.0 (C(4d)).

[(dmap)Me_2Al–P($SiMe_3$)$_2$–Cr$(CO)_5$] (3): [(Me_3N)Cr$(CO)_5$] (1.1 mmol, 0.26 g) was added to a solution of [(dmap)Me_2Al–P($SiMe_3$)$_2$] (1.0 mmol, 0.36 g) in hexane (15 mL), and the resulting intensely yellow solution was heated under reflux for 1 h. The product separated as a yellow solid that was filtered and washed with hexane (5 mL). Recrystallization from CH_2Cl_2 at 0 °C gave yellow crystals of X-ray quality. Yield (crude product): 0.49 g (0.89 mmol, 89 %); m.p. 155–165 °C (dec); ^{1}H NMR (300 MHz, CD_2Cl_2, −10 °C): $\delta = -0.49$ (d, $^3J_{PH} = 2.2$ Hz, 6H; $AlMe_2$), 0.32 (d, $^3J_{PH} = 4.4$ Hz, 18H; $SiMe_3$), 3.11 (s, 6H; NMe_2), 6.64 (d, $^2J_{HH} = 7.2$ Hz, 2H; C(3d)–H), 8.06 (d, $^2J_{HH} = 7.4$ Hz, 2H; C(2d)–H); ^{13}C{^{1}H} NMR (75.5 MHz, CD_2Cl_2, −10 °C): $\delta = -5.1$ (d, $^2J_{PC} = 13.6$ Hz; $AlMe_2$), 4.2 (d, $^2J_{PC} = 7.1$ Hz; $SiMe_3$), 39.7 (NMe_2), 107.1 (C(3d)–H), 146.5 (C(2d)–H), 156.0 (C(4d)), 217.8 (d, $^2J_{PC} = 8.4$ Hz; *cis*-CO), 223.7 (d, $^2J_{PC} = 4.8$ Hz; *trans*-CO); ^{31}P{^{1}H} NMR (121.5 MHz, CH_2Cl_2, 30 °C): $\delta = -278.1$; IR (CH_2Cl_2): $\tilde{\nu} = 1929$ (ν_{CO}, E), 2027, 2056 cm^{-1} (ν_{CO}, A_1).

[(dmap)Me_2Al–As($SiMe_3$)$_2$–Cr$(CO)_5$] (4): [(Me_3N)Cr$(CO)_5$] (1.1 mmol, 0.26 g) was added to a solution of [(dmap)Me_2Al–As($SiMe_3$)$_2$] (1.0 mmol, 0.40 g) in hexane (10 mL), and the resulting orange solution was heated under reflux for 1 h. The product separated as a reddish solid that was filtered and washed with hexane (5 mL). Recrystallization from CH_2Cl_2 at 0 °C gave yellow crystals of X-ray quality. Yield (crude product): 0.45 g (0.76 mmol, 76 %); m.p. 150–155 °C (dec); ^{1}H NMR (300 MHz, CD_2Cl_2, −10 °C): $\delta = -0.47$ (s, 6H; $AlMe_2$), 0.35 (s, 18H; $SiMe_3$), 3.11 (s, 6H; NMe_2), 6.65 (d, $^2J_{HH} = 7.4$ Hz, 2H; C(3d)–H), 8.05 (d, $^2J_{HH} = 6.8$ Hz, 2H; C(2d)–H); ^{13}C{^{1}H} NMR (75.5 MHz, CD_2Cl_2, −10 °C): $\delta = -5.6$ ($AlMe_2$), 4.1 ($SiMe_3$), 39.7 (NMe_2), 107.1 (C(3d)–H), 146.2 (C(2d)–H), 156.0 (C(4d)), 219.7 (*cis*-CO), 225.1 (*trans*-CO); IR (CH_2Cl_2): $\tilde{\nu} = 1921$ (ν_{CO}, E), 2025, 2044 cm^{-1} (ν_{CO}, A_1).

[(dmap)Me_2Al–P($SiMe_3$)$_2$–Fe$(CO)_4$] (5): [(dmap)Me_2Al–P($SiMe_3$)$_2$] (1.0 mmol, 0.36 g) was added to a solution of $[Fe_3(CO)_{12}]$ (0.33 mmol, 0.17 g) in hexane (50 mL). The initial dark green solution turned brownish

orange within 30 min. The solution was separated from some dark red by-product and cooled to −60 °C for 48 h to yield yellow crystals suitable for an X-ray structure analysis. Yield: 0.10 g (0.19 mmol, 19 %); m.p. 82–86 °C (red oil); ^{1}H NMR (300 MHz, [D$_8$]toluene, 30 °C): $\delta = -0.10$ (br, 6H; $AlMe_2$), 0.56 (d, $^3J_{PH} = 5.6$ Hz, 18H; $SiMe_3$), 2.11 (s, 6H; NMe_2), 5.83 (br, 2H; C(3d)−H), 7.96 (br, 2H; C(2d)−H); ^{13}C{^{1}H} NMR (75.5 MHz, [D$_8$]toluene, 30 °C): $\delta = -8.1$ (br s, $AlMe_2$), 2.1 (d, $^2J_{PC} = 7.1$ Hz; $SiMe_3$), 38.3 (NMe_2), 106.9 (C(3d)−H), 146.4 (C(2d)−H), 155.9 (C(4d)), 215.3 (d, $^2J_{PC} = 13.3$ Hz; *cis*-CO), 216.9 (d, $^2J_{PC} = 13.6$ Hz; *trans*-CO); ^{31}P{^{1}H} NMR (121.5 MHz, [D$_8$]toluene, 30 °C): $\delta = -258.4$; IR (CH_2Cl_2): $\tilde{\nu} = 1911$ (ν_{CO}, E), 1956, 2008 cm^{-1} (ν_{CO}, A_1).

[(dmap)Me$_2$Al−P(SiMe$_3$)$_2$−Ni(CO)$_3$] (6): [Ni(CO)$_4$] (0.75 mmol, 0.1 mL) was added to a solution of [(dmap)Me$_2$Al−P(SiMe$_3$)$_2$] (0.5 mmol, 0.18 g) in cyclohexane (5 mL). Rapid gas evolution was observed, and the solution was stirred at room temperature for 30 min. The yellow solution was separated from some dark by-product and cooled to 0 °C to yield colorless crystals suitable for an X-ray structure analysis. Yield: 0.17 g (0.34 mmol, 68 %); m.p. 102–110 °C (dec); ^{1}H NMR (200 MHz, C_6D_6, 30 °C): $\delta = -0.02$ (d, $^3J_{PH} = 2.6$ Hz, 6H; $AlMe_2$), 0.47 (d, $^3J_{PH} = 4.6$ Hz, 18H; $SiMe_3$), 1.87 (s, 6H; NMe_2), 5.71 (d, $^3J_{HH} = 7.4$ Hz, 2H; C(3d)−H), 8.09 (d, $^3J_{HH} = 7.4$ Hz, 2H; C(2d)−H); ^{13}C{^{1}H} NMR (50 MHz, C_6D_6, 30 °C): $\delta = -6.1$ (d, $^2J_{PC} = 16.1$ Hz; $AlMe_2$), 3.4 (d, $^2J_{PC} = 8.4$ Hz; $SiMe_3$), 38.5 (NMe_2), 107.0 (C(3d)−H), 146.6 (C(2d)−H), 155.9 (C(4d)), 199.5 (d, $^2J_{PC} = 1.6$ Hz; CO); ^{31}P{^{1}H} NMR (121.5 MHz, C_6D_6, 30 °C): $\delta = -275.2$; IR (pentane): $\tilde{\nu} = 1961$, 1975 (ν_{CO}, E), 2048 cm^{-1} (ν_{CO}, A_1).

General preparation of [(dmap)Me$_2$Ga−E(SiMe$_3$)$_2$−Ni(CO)$_3$]: At 0 °C, [Ni(CO)$_4$] (0.75 mmol, 0.1 mL) was added to a solution of [(dmap)Me$_2$M−E(SiMe$_3$)$_2$] (0.5 mmol; E = P: 0.20 g; E = As: 0.22 g, E = Sb: 0.25 g) in pentane (20 mL). A smooth gas evolution was observed, and the resulting suspension was slowly warmed to room temperature. The slightly brown solution was separated from some dark by-product and cooled to −30 °C to yield colorless crystals suitable for an X-ray structure analysis.

[(dmap)Me$_2$Ga−P(SiMe$_3$)$_2$−Ni(CO)$_3$] (7): Yield: 0.24 g (0.44 mmol, 89 %); m.p. 100–120 °C (dec); ^{1}H NMR (300 MHz, C_6D_6, 30 °C): $\delta = 0.29$ (d, $^3J_{PH} = 3.0$ Hz, 6H; $GaMe_2$), 0.44 (d, $^3J_{PH} = 4.7$ Hz, 18H; $SiMe_3$), 1.92 (s, 6H; NMe_2), 5.77 (dd, $^3J_{HH} = 5.7$ Hz, $^4J_{HH} = 1.5$ Hz, 2H; C(3d)−H), 8.05 (dd,

Table 4. Crystal data and structure refinement for the DMAP-coordinated gallanes **1** and **2**.

	1	**2**
formula	$C_{15}H_{34}GaN_2PSi_2$	$C_{15}H_{34}AsGaN_2Si_2$
M_r	399.31	443.26
T [K]	123(2)	123(2)
λ [Å]	0.71073 ($Mo_{K\alpha}$)	0.71073 ($Mo_{K\alpha}$)
crystal system	monoclinic	monoclinic
space group	$P2_1/n$ (no. 14)	$P2_1/c$ (no. 14)
unit cell dimensions, a [Å]	15.1439(3)	15.1022(2)
b [Å]	9.0238(2)	9.0983(2)
c [Å]	17.5573(5)	17.6064(4)
$\alpha = \gamma$ [°]	90	90
β [°]	115.527(1)	115.171(1)
V [Å^3]	2165.09(9)	2189.47(8)
Z, ρ_{calcd} [g cm^{-3}]	4, 1.225	4, 1.345
μ [mm^{-1}]	1.453	2.863
crystal size [mm^3]	0.25 × 0.20 × 0.10	0.60 × 0.60 × 0.50
absorption correction	empirical from multiple refl.	empirical from multiple refl.
max/min transmission	0.9400/0.6634	0.3294/0.2787
θ range for data collection [°]	2.98–25.00	2.98–25.00
refl. collected/unique	29245/3760 ($R_{int} = 0.0962$)	18905/3834 ($R_{int} = 0.0573$)
refined parameters	192	192
goodness of fit on F^2	0.974	1.056
final $R1$ indices [$I > 2\sigma(I)$]	0.0286	0.0226
$wR2$ indices (all data)	0.0739	0.0617
resid. electron dens. [e Å^{-3}]	0.511/−0.480	0.392/−0.389

Table 5. Crystal data and structure refinement for the Al-containing complexes **3**, **4**, **5**, and **6**.

	3	**4**	**5**	**6**
formula	$C_{20}H_{34}AlCrN_2O_5PSi_2$	$C_{20}H_{34}AlAsCrN_2O_5Si_2$	$C_{19}H_{34}AlFeN_2O_4PSi_2$	$C_{18}H_{34}AlN_2NiO_3PSi_2$
M_r	548.62	592.57	524.46	499.31
T [K]	123(2)	123(2)	123(2)	123(2)
λ [Å]	0.71073 ($Mo_{K\alpha}$)	0.71073 ($Mo_{K\alpha}$)	0.71073 ($Mo_{K\alpha}$)	0.71073 ($Mo_{K\alpha}$)
crystal system	triclinic	triclinic	triclinic	triclinic
space group	$P\bar{1}$ (no. 2)	$P\bar{1}$ (no. 2)	$P\bar{1}$ (no. 2)	$P\bar{1}$ (no. 2)
unit cell dimensions, a [Å]	9.6557(1)	9.6747(2)	8.9010(1)	14.1108(5)
b [Å]	9.8037(2)	9.8384(2)	9.8998(2)	22.0283(6)
c [Å]	15.5468(3)	15.6495(3)	17.8311(3)	27.8303(11)
α [°]	89.699(1)	89.587(1)	78.696(1)	103.184(2)
β [°]	72.641(1)	72.754(1)	80.277(1)	99.791(2)
γ [°]	89.125(1)	89.494(1)	64.428(1)	99.553(2)
V [Å^3]	1404.49(4)	1422.53(5)	1383.51(4)	8108.8(5)
Z, ρ_{calcd} [g cm^{-3}]	2, 1.297	2, 1.383	2, 1.259	12, 1.227
μ [mm^{-1}]	0.611	1.701	0.746	0.917
crystal size [mm^3]	0.30 × 0.12 × 0.06	0.30 × 0.20 × 0.15	0.35 × 0.20 × 0.08	0.50 × 0.20 × 0.10
absorption correction	none	empirical from multiple refl.	empirical from multiple refl.	empirical from multiple refl.
max/min transmission		0.8109/0.5949	0.8528/0.7928	0.8929/0.8438
θ range for data collect. [°]	2.93–25.00	2.92–25.00	2.64–25.00	1.50–25.04
refl. collected/unique	27758/4905 ($R_{int} = 0.0527$)	28299/4991 ($R_{int} = 0.0545$)	23708/4861 ($R_{int} = 0.0488$)	44477/25286 ($R_{int} = 0.0801$)
refined parameters	291	291	273	1525
goodness of fit on F^2	1.028	1.016	1.008	0.770
final $R1$ indices [$I > 2\sigma(I)$]	0.0354	0.0237	0.0278	0.0508
$wR2$ indices (all data)	0.0984	0.0575	0.0710	0.1099
resid. electron dens. [e Å^{-3}]	0.569/−0.374	0.402/−0.410	0.358/−0.207	0.386/−0.474

0947-6539/02/0808-1922 $ 20.00+.50/0 *Chem. Eur. J.* **2002**, *8*, No. 8

$^3J_{HH} = 5.7$ Hz, $^4J_{HH} = 1.5$ Hz, 2H; C(2d)–H); $^{13}C\{^1H\}$ NMR (75.5 MHz, C_6D_6, 30 °C): $\delta = -3.1$ (d, $^2J_{PC} = 17.1$ Hz; $GaMe_2$), 3.3 (d, $^2J_{PC} = 8.4$ Hz; $SiMe_3$), 38.1 (NMe_2), 106.6 (C(3d)–H), 146.8 (C(2d)–H), 155.2 (C(4d)), 199.5 (d, $^2J_{PC} = 1.6$ Hz; CO); ^{31}P NMR (121.5 MHz, C_6D_6, 30 °C): $\delta = -260.8$; IR (pentane): $\tilde{\nu} = 1965$, 1975 (ν_{CO}, E), 2050 cm^{-1} (ν_{CO}, A_1).

[(dmap)Me_2Ga–As($SiMe_3$)$_2$–Ni(CO)$_3$] (8): Yield: 0.27 g (0.46 mmol, 92 %); m.p. 115–120 °C (dec); ^1H NMR (300 MHz, C_6D_6, 30 °C): $\delta = 0.30$ (s, 6H; $GaMe_2$), 0.47 (s, 18H; $SiMe_3$), 1.95 (s, 6H; NMe_2), 5.65 (dd, $^3J_{HH} = 5.7$ Hz, $^4J_{HH} = 1.5$ Hz, 2H; C(3d)–H), 7.88 (dd, $^3J_{HH} = 5.7$ Hz, $^4J_{HH} = 1.5$ Hz, 2H; C(2d)–H); $^{13}C\{^1H\}$ NMR (75.5 MHz, C_6D_6, 30 °C): $\delta = -3.0$ ($GaMe_2$), 3.5 ($SiMe_3$), 38.1 (NMe_2), 106.7 (C(3d)–H), 146.6 (C(2d)–H), 155.3 (C(4)), 199.6 (CO); IR (pentane): $\tilde{\nu} = 1961$, 1973 (ν_{CO}, E), 2048 cm^{-1} (ν_{CO}, A_1).

[(dmap)Me_2Ga–Sb($SiMe_3$)$_2$–Ni(CO)$_3$] (9): Yield: 0.26 g (0.41 mmol, 82 %); m.p. 72–76 °C (dec); ^1H NMR (300 MHz, C_6D_6, 30 °C): $\delta = 0.36$ (s, 6H; $GaMe_2$), 0.53 (s, 18H; $SiMe_3$), 1.97 (s, 6H; NMe_2), 5.65 (d, $^3J_{HH} = 7.2$ Hz, 2H; C(3d)–H), 7.96 (br, 2H; C(2d)–H); $^{13}C\{^1H\}$ NMR (75.5 MHz, C_6D_6, 30 °C): $\delta = -2.2$ ($GaMe_2$), 3.5 ($SiMe_3$), 38.1 (NMe_2), 106.7 (C(3d)–H), 146.6 (C(2d)–H), 155.3 (C(4)), 200.7 (CO); IR (pentane): $\tilde{\nu} = 1961$, 1973 (ν_{CO}, E), 2044 cm^{-1} (ν_{CO}, A_1).

X-ray structure solution and refinement: Crystallographic data of **1**–**6**, **8**, and **9** are summarized in Tables 4, 5, and 6. Figures 1 to 8 show the ORTEP diagrams (50 % probability ellipsoids, ball-and-stick model for **6**) of the solid-state structures of the compounds. Selected bond lengths and angles are summarized in Tables 1 and 2. Data were collected on a Nonius KappaCCD diffractometer. The structures were solved by Patterson methods (SHELXS-97)[28] and refined by full-matrix least-squares analysis on F^2 (full-matrix-block least-squares analysis on F^2 for **6**). Except for **3**, empirical absorption corrections were applied. All non-hydrogen atoms were refined anisotropically, and hydrogen atoms by a riding model (SHELXL-97).[29]

CCDC-171404 (**1**), CCDC-171405 (**2**), CCDC-171406 (**3**), CCDC-171407 (**4**), CCDC-171408 (**5**), CCDC-171409 (**6**), CCDC-171410 (**8**), and CCDC-171411 (**9**) contain the supplementary crystallographic data for this paper. These data can be obtained free of charge via www.ccdc.cam.ac.uk/conts/retrieving.html (or from the Cambridge Crystallographic Data Centre, 12 Union Road, Cambridge CB2 1EZ, UK; fax: (+44) 1223-336-033; or e-mail: deposit@ccdc.cam.ac.uk).

Table 6. Crystal data and structure refinement for the Ga-containing complexes **8** and **9**.

	8	**9**
formula	$C_{18}H_{34}AsGaN_2NiO_3Si_2$	$C_{18}H_{34}GaN_2NiO_3SbSi_2$
M_r	586.00	632.83
T [K]	123(2)	123(2)
λ [Å]	0.71073 ($Mo_{K\alpha}$)	0.71073 ($Mo_{K\alpha}$)
crystal system	triclinic	triclinic
space group	$P\bar{1}$ (no. 2)	$P\bar{1}$ (no. 2)
unit cell dimensions, a [Å]	9.0496(1)	9.2015(2)
b [Å]	9.3461(1)	9.4247(2)
c [Å]	17.3815(4)	17.4841(3)
α [°]	101.262(1)	101.694(1)
β [°]	94.609(1)	94.604(1)
γ [°]	108.005(1)	107.611(1)
V [Å^3]	1355.49(4)	1398.81(5)
Z, ρ_{calcd} [g cm^{-3}]	2, 1.436	2, 1.502
μ [mm^{-1}]	3.006	2.684
crystal size [mm^3]	0.45 × 0.20 × 0.10	0.35 × 0.20 × 0.10
absorption correction	empirical from multiple refl.	empirical from multiple refl.
max/min transmission	0.4796/0.3671	0.6575/0.5728
θ range for data collection [°]	2.84–25.00	2.80–25.00
refl. collected/unique	22624/4752 ($R_{int} = 0.0615$)	18343/4784 ($R_{int} = 0.0411$)
refined parameters	255	255
goodness of fit on F^2	1.038	1.041
final $R1$ indices [$I > 2\sigma(I)$]	0.0226	0.0190
$wR2$ indices (all data)	0.0573	0.0456
resid. electron dens. [e Å^{-3}]	0.433/–0.352	0.313/–0.541

Acknowledgements

S. Schulz gratefully acknowledges financial support by the DFG, the Fonds der Chemischen Industrie, the Bundesministerium für Bildung und Forschung, (BMBF) and Prof. E. Niecke (Universität Bonn). F. Thomas would like to thank the Fonds der Chemischen Industrie for a fellowship award, M. Nieger thanks the Deutscher Akademischer Austauschdienst (DAAD), and K. Nättinen thanks the Academy of Finland for financial support.

[1] See for example: a) A. H. Cowley, R. A. Jones, *Angew. Chem.* **1989**, *101*, 1235; *Angew. Chem. Int. Ed. Engl.* **1989**, *28*, 1208; b) P. O'Brien, S. Haggata, *Adv. Mater. Opt. Electron.* **1995**, *5*, 117; c) A. C. Jones, *Chem. Soc. Rev.* **1997**, 101; d) A. C. Jones, P. O'Brien, *CVD of Compounds Semiconductors: Precursor Synthesis, Development and Applications*, VCH, Weinheim, **1997**.

[2] a) P. P. Power, *Chem. Rev.* **1999**, *99*, 3463, and references therein; b) H.-J. Himmel, A. J. Downs, T. M. Greene, *Chem. Commun.* **2000**, 871; c) H.-J. Himmel, A. J. Downs, J. C. Green, T. M. Greene, *J. Chem. Soc. Dalton Trans.* **2001**, 535; d) N. J. Hardman, C. M. Cui, H. W. Roesky, W. H. Fink, P. P. Power, *Angew. Chem.* **2001**, *113*, 2230; *Angew. Chem. Int. Ed.* **2001**, *40*, 2172. In the present manuscript Group 13 elements are referred to as triel and Group 15 elements as pentel in accordance with an IUPAC suggestion: J. Falbe, M. Regitz, *Römpp Chemie Lexikon*, *Vol. 4*, Georg-Thieme, Stuttgart, **1995**, p. 3282.

[3] C. Tessier-Youngs, C. Bueno, O. T. Beachley, Jr., M. R. Churchill, *Inorg. Chem.* **1983**, *22*, 1054. During the preparation of this manuscript, Scheer et al. described the single-crystal X-ray structures of the Lewis acid/base-stabilized phosphanylalane and -gallane $[Me_3N(H)_2M{-}P(H_2){-}W(CO)_5]$ (M = Al, Ga), which were obtained by reaction of $Me_3N{-}MH_3$ and $H_3P{-}W(CO)_5$. Computational calculations confirmed both the Lewis acid $[W(CO)_5]$ and the Lewis base Me_3N to be essential for the stabilization of monomeric phosphanylalane and gallane. U. Vogel, A. Y. Timoshkin, M. Scheer, *Angew. Chem.* **2001**, *113*, 4541; *Angew. Chem. Int. Ed.* **2001**, *40*, 4409.

[4] Beachley et al. reported the synthesis of compounds of the type $[Me_3N(t\mathrm{BuCH}_2)_2M{-}P(Ph_2){-}Cr(CO)_5]$ (M = Al, Ga) and $Et_4N[(Me_3SiCH_2)_2M(Cl){-}P(Ph_2){-}M'(CO)_5]$ (M = Ga, In; M′ = Cr, Mo, W), but in most cases only ^{31}P NMR and IR spectral data are specified. None of these compounds were characterized by X-ray structure analysis. O. T. Beachley, Jr., M. A. Banks, J. P. Kopasz, R. D. Rogers, *Organometallics* **1996**, *15*, 5170.

[5] a) S. Schulz, M. Nieger, *Organometallics* **2000**, *19*, 2640; b) A. Kuczkowski, F. Thomas, S. Schulz, M. Nieger, *Organometallics* **2000**, *19*, 5758; c) F. Thomas, S. Schulz, M. Nieger, *Eur. J. Inorg. Chem.* **2001**, 161.

[6] F. Thomas, S. Schulz, M. Nieger, *Organometallics* **2001**, *20*, 2405.

[7] F. Thomas, S. Schulz, unpublished results.

[8] a) M. D. B. Dillingham, J. A. Burns, J. Byers-Hill, K. D. Gripper, W. T. Pennington, G. H. Robinson, *Inorg. Chim. Acta* **1994**, *216*, 267; b) D. Wiedmann, H. D. Hausen, J. Weidlein, *Z. Anorg. Allg. Chem.* **1995**, *621*, 1351; c) A. Schaller, H. D. Hausen, W. Schwarz, G. Heckmann, J. Weidlein, *Z. Anorg. Allg. Chem.* **2000**, *626*, 1047.

[9] Cambridge Structural Database (version 5.21, April 2001); F. H. Allen, O. Kennard, *Chem. Design Automation News* **1993**, *8*, 31.
[10] A. F. Holleman, E. Wiberg, *Lehrbuch der Anorganischen Chemie (101. Aufl.)*, W. de Gruyter, Berlin, **1995**, p. 1838.
[11] a) J. L. Atwood, S. G. Bott, F. M. Elms, C. Jones, C. L. Raston, *Inorg. Chem.* **1991**, *30*, 3792; b) J. L. Atwood, S. G. Bott, M. G. Gardiner, C. Jones, G. A. Koutsantonis, C. L. Raston, K. D. Robinson, *Inorg. Chem.* **1993**, *32*, 3482.
[12] J. J. Byers, W. T. Pennington, G. H. Robinson, *Acta Crystallogr. Sect. C* **1992**, *48*, 2023.
[13] Y. Koide, J. A. Francis, S. G. Bott, A. R. Barron, *Polyhedron* **1998**, *17*, 983.
[14] A. Haaland, *Angew. Chem.* **1989**, *101*, 1017; *Angew. Chem. Int. Ed. Engl.* **1989**, *28*, 992.
[15] G. M. Bodner, M. P. May, L. E. McKinney, *Inorg. Chem.* **1980**, *19*, 1951.
[16] a) A. J. Carty, N. J. Taylor, A. W. Coleman, M. F. Lappert, *J. Chem. Soc. Chem. Commun.* **1979**, 639; b) H. J. Plastas, J. M. Steward, S. O. Grim, *Inorg. Chem.* **1973**, *12*, 265.
[17] L. Weber, M. H. Scheffer, H.-G. Stammler, B. Neumann, *Eur. J. Inorg. Chem.* **1998**, 55.
[18] See for example C. van Wüllen, *J. Comput. Chem.* **1997**, *18*, 1985, and references therein.
[19] Y. Chen, M. Hartmann, G. Frenking, *Z. Anorg. Allg. Chem.* **2001**, *627*, 985, and references therein.
[20] L. Weber, R. Kirchhoff, R. Boese, *J. Chem. Soc. Chem. Commun.* **1992**, 1182.
[21] J. Pickardt, L. Rösch, H. Schumann, *Z. Anorg. Allg. Chem.* **1976**, *426*, 66.
[22] $\chi = \nu\{A_1,\ [(L)Ni(CO)_3]\} - \nu\{A_1,\ [(tBu_3P)Ni(CO)_3]\}$. C. A. Tolman, *Chem. Rev.* **1977**, *77*, 313.
[23] T. Bartik, T. Himmler, H.-G. Schulte, K. Seevogel, *J. Organomet. Chem.* **1985**, *293*, 343.
[24] Electronegativities according to Allred – Rochow. A. F. Holleman, E. Wiberg, *Lehrbuch der Anorganischen Chemie (101. Aufl.)*, W. de Gruyter, Berlin, **1995**, p. 144.
[25] The band splitting of the E vibration is likely to be due to the disturbance of the local C_{3v} symmetry of the $[(L)Ni(CO)_3]$ fragment. This has been already observed for the analogous aluminum compounds.[6]
[26] Since the molecular structure of $[(dmap)Me_2Ga{-}Sb(SiMe_3)_2]$ has not been determined so far, all comparisons refer to the ethyl derivative $[(dmap)Et_2Ga{-}Sb(SiMe_3)_2]$.[5c]
[27] M. S. Davies, R. K. Pierens, M. J. Aroney, *J. Organomet. Chem.* **1993**, *458*, 141.
[28] G. M. Sheldrick, SHELXS-97, Program for the Solution of Crystal Structures, University of Göttingen (Germany); G. M. Sheldrick, *Acta Crystallogr. Sect. A* **1990**, *46*, 467.
[29] G. M. Sheldrick, SHELXL-97, Program for Crystal Structure Refinement, University of Göttingen (Germany), **1997**.

Received: October 4, 2001 [F3588]

  0947-6539/02/0808-1924 $ 20.00+.50/0